The influence of anisotropic voxel caused by field of view setting on the accuracy of three-dimensional reconstruction of bone geometric models

Yaming Liu, Ruining Li, Yuxuan Fan, Đorđe Antonijević, Petar Milenković, Zhiyu Li, Marija Djuric, and Yifang Fan

Citation: AIP Advances **8**, 085111 (2018); doi: 10.1063/1.5041990
View online: https://doi.org/10.1063/1.5041990
View Table of Contents: http://aip.scitation.org/toc/adv/8/8
Published by the American Institute of Physics

The influence of anisotropic voxel caused by field of view setting on the accuracy of three-dimensional reconstruction of bone geometric models

Yaming Liu,[1] Ruining Li,[1] Yuxuan Fan,[1] Đorđe Antonijević,[1,2]
Petar Milenković,[3,4] Zhiyu Li,[5] Marija Djuric,[3] and Yifang Fan[1,a]
[1]*School of Physical Education and Sport Science, Fujian Normal University, Fuzhou 350108, Fujian, China*
[2]*Laboratory for Atomics Physics, Institute for Nuclear Sciences "Vinca," University of Belgrade, 11000 Belgrade, Serbia*
[3]*Laboratory for Anthropology, Institute of Anatomy, School of Medicine, University of Belgrade, 11000 Belgrade, Serbia*
[4]*Institute of Oncology and Radiology of Serbia–National Cancer Research Center, 11000 Belgrade, Serbia*
[5]*College of Foreign Studies, Jinan University, Guangzhou 510632, Guangdong, China*

(Received 29 May 2018; accepted 7 August 2018; published online 16 August 2018)

The finite element method is playing an increasingly important role in osteoporosis screening. An accurate bone geometric model, a prerequisite for the finite element analysis, is affected by voxels. Isotropic voxel has advantages in three-dimensional reconstruction, but field of view setting usually results in anisotropic voxels. The main goal of this study was to investigate the influence of anisotropic voxel on the accuracy of three-dimensional reconstruction of bone geometric models. Sixty metatarsal bones were scanned twice with an interval of 18 months with different fields of view. We reconstructed these metatarsals and compared them. The results showed that there was no significant difference in volume, surface, length, width and height and two principal moments of inertia, indicating that anisotropic voxel caused by field of view setting has a neglectable effect on the three-dimensional reconstruction of bone geometric models, and that using finite element method based on bone geometric model reconstructed by anisotropic voxel to predict bone strength is reliable.
https://doi.org/10.1063/1.5041990

I. INTRODUCTION

World Health Organization technical report estimated that about 200 million people suffer from osteoporosis,[1] and about 9 million experience fracture annually.[2] The International Osteoporosis Foundation Compendium of Osteoporosis reported that 158 million people aged 50 years or older were regarded as high-risk group of fractures caused by osteoporotic in 2010, and the number would be doubled in 2040.[3] Fractures, especially hip fractures, have been a major public health problem.[4] And the number of fractures has been increasing.[5] Therefore, it is suggested that women aged 65 years or older and men aged over 70 years should undertake osteoporosis screening.[6] In screening, bone mineral density (BMD) measured by dual energy X-ray absorptiometry (DXA) is regarded as the gold standard for osteoporosis screening.[7] The quantitative computed tomography (QCT) has also been enrolled in osteoporosis screening recently.[8–10] But a growing number of studies found that osteoporosis screening based on BMD did not significantly influenced fracture incidence, as

[a]Corresponding author Professor Yifang Fan E-mail: tfyf@fjnu.edu.cn. School of Physical Education and Sport Science Fujian Normal University Fuzhou, Fujian, China

well as morbidity or mortality associated with fracture.[4,11–14] In addition to DXA and QCT, more researchers tend to use the finite element analysis (FEA) method to investigate bone features,[4,15–18] since FEA reveals information of the three-dimensional (3D) morphology, the material property and the loading distribution of bone, which may provide a more accurate bone strength prediction.[4,16,17,19–23] Among all factors that affect FEA analysis results, a critical one is bone geometric model.[22]

Digital Imaging and Communications in Medicine (DICOM) is the international standard of medical imaging. Digital imaging refers to successive two-dimensional slices derived from CT and MRI, i.e. a data set of data elements. The length and width of a data element (also called slice pixel) are the same as those of a voxel.[24] The length and width of a voxel can be calculated by the following formulas respectively: voxel length=FOV(mm)/slices length (px) and voxel width=FOV(mm)/slices width (px).[25] The height of a voxel is the vertical distance between two slices, which can also be called as slice increment. When the length, width and height are identical, the voxel is isotropic; when they are not, the voxel is anisotropic. Thus, FOV setting is one critical factor that determines whether a voxel is isotropic or anisotropic.

The quality of cross section image (CSI) is an important factor affecting the accuracy of bone geometric model.[26,27] Isotropic voxel has advantages in the quality of the reconstruction of geometric model.[28–32] For instance, the use of submillimeter isotropic datasets in heart, lungs and musculoskeletal imaging has proven to be beneficial.[33–37] Spiral CT scanner can provide isotropic data.[38] Unfortunately, to ensure the region-of-interest (ROI) of bone to be fully rendered at field of view (FOV) with high resolution, the size of the FOV needs to be adjusted, which leads to the fact that the slice pixel is not consistent with the slice increment, i.e. anisotropic voxel is produced. It remains unclear to what degree the anisotropic voxels set by different FOVs might influence the accuracy of the bone geometric model.

In the present paper, we hypothesize that the anisotropic voxels generated by different FOVs do not have a significant effect on the reconstruction of bone geometric model. To verify our hypothesis, 6 participants' foot bones were scanned twice (with an interval of 18 months) with different FOVs and several linear, volumetric and kinematic parameters in generated models were compared. One hundred and twenty metatarsals from these two scans were reconstructed and their geometric models were generated. After comparing the reconstructed models, we found that there was no significant difference in the volume, surface, length, width and height nor in bones' two principal moments of inertia (PMIs). At the sub-millimeter scale, the reconstructed bone geometric models derived from anisotropic voxels are accurate, indicating that applying the reconstructed bone geometric model generated by anisotropic voxels to finite element analysis is reliable.

II. SUBJECTS AND METHODS

A. Subjects

The study was approved by the Ethical Committee of Fujian Normal University. Six male subjects without injury or skeletal muscle disease (mean age:25±3years; mean height: 171±5cm; mean weight: 66±5kg) were recruited. Their foot bone was scanned twice, with an interval of 18 months. Altogether, 120 metatarsal bone data were collected and analyzed. The tests were carried out in accordance with the approved guidelines. All subjects provided fully informed consent to participate in this study by signing a written consent form.

B. Data acquisition

Both scans were performed with the same multi-slice CT scanner (Philips/Brilliance 64). The scanner settings were the same for both examinations: approximately 120kVp and 50 mA. The scanning was conducted along with both foot transects, from top to bottom. Participants were asked to remain in the standard anatomical position. CT images were reconstructed by the scan condition of bone window, 0.9 mm slice thickness with 0.45mm slice increment, 768*768 pixels. CT DICOM format data were input into Mimics software, which were then used to create 3D geometric model of metatarsals. See Part I of the supplementary material for slice parameter information.

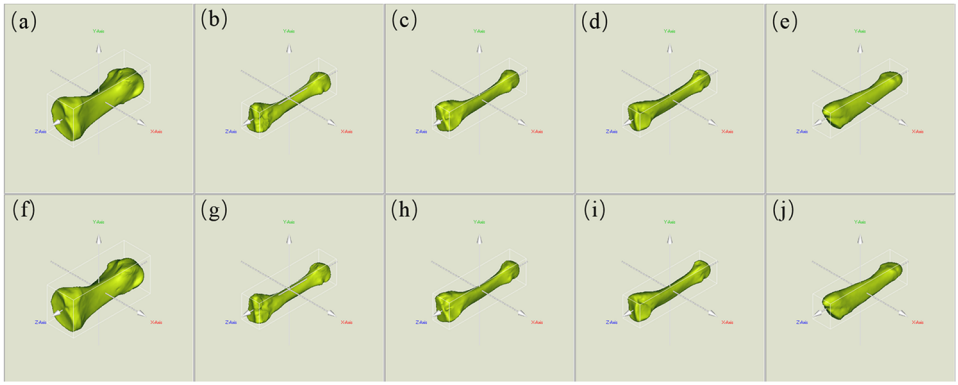

FIG. 1. Bone's coordinate system. (a)-(e) the bone's coordinate system of the 1st to the 5th metatarsal bones from the first scan. (f)-(j) the bone's coordinate system of the 1st to the 5th metatarsal bones from the second scan. (See Part IV of the supplementary material for the positioned body coordinate systems of 120 metatarsals.)

C. Three-dimensional modeling of the metatarsals

Different scanning postures may change the metatarsals' body coordinate systems. (See Part II of the supplementary material for the original body coordinate systems of 120 metatarsals.) To eliminate the effect caused by different scanning postures, we used the center of mass (COM) as the origin of the bone's body coordinate system) and three bone principal axes of inertia (PAIs) as the bone's body coordinate axes. See Fig. 1. The positioning method was described fully in Part III of the supplementary material (In this study, all metatarsals were positioned by rotating around axis $x \to y \to z \to x \to y \to z \cdots$, accordingly).

The following parameters of the metatarsal were obtained based on the body coordinate system of bone: the length, width, height, gray values, surface, volume, and three PMIs around *x, y* and *z* axis, respectively. The following equation was used to standardize these three PMIs.

$$\begin{cases} I_x = \dfrac{I_x}{I_x + I_y + I_z} \times 100 \\ I_y = \dfrac{I_y}{I_x + I_y + I_z} \times 100 \\ I_z = \dfrac{I_z}{I_x + I_y + I_z} \times 100 \end{cases} \tag{1}$$

where I_x, I_y and I_z refer to PMI around x, y and z axis of the bone, respectively.

Statistical analyses were performed using the SPSS software system (version 17). In all analyses, the significance level was set at 0.05. The data were tested for normality of distribution by Kolmogorov–Smirnov test. The paired sample t test was employed to compare the measured length, width, height, gray value, volume, surface and PMIs around x, y and z axis of the geometric model of 120 metatarsals.

III. RESULTS

The metatarsals' positioning from two scans is shown in FIG 2.

The length, width and height of metatarsal bones from both scans are shown in Part V of the supplementary material (Table 2A). The paired sample t test was employed to compare the measured length, width and height of the geometric model of 120 metatarsals. The results showed that different sizes of anisotropic voxels had no significant difference in length, width and height of bone geometric models from two scans ($P > 0.05$).

The variation of length, width and height of metatarsals is shown in Part V of the supplementary material (Table 2B). We compared the variation of length, width and height of the bone geometric

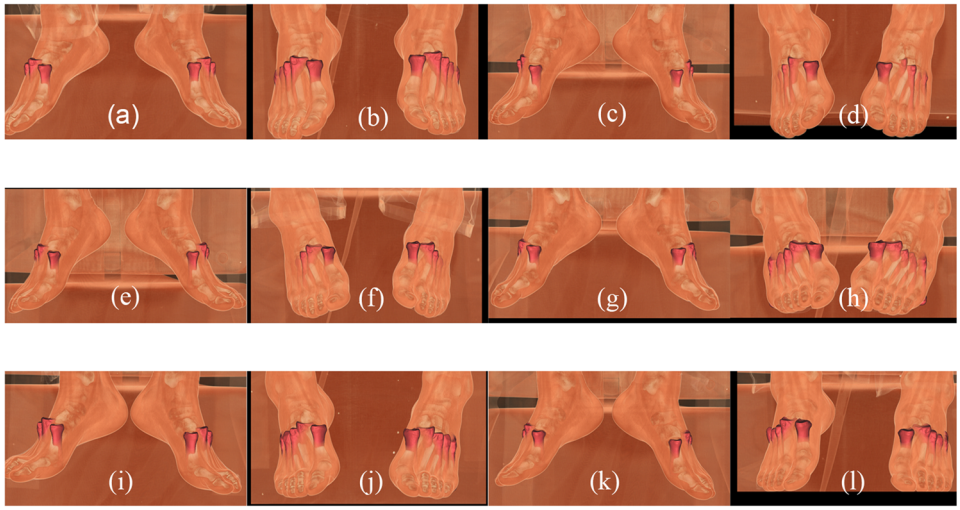

FIG. 2. Results from metatarsals' positioning of six participants (two scans), respectively presented for each subject. (a) (c) (e) (g) (i) (k) the metatarsals' positioning of the first scan of the six participants. (b) (d) (f) (h) (j) (l) the metatarsals' positioning of the second scan of the six participants.

models – they were mostly smaller than those of the pixel resolution and slice increment. The variation ratio of bone length from two scans is shown in Part IV of the supplementary material (Table 2C), which demonstrated the length discrepancy between two scans below 1%.

The bone volume, surface and gray values of metatarsal bones from both scans are shown in Part V of the supplementary material (Table 3). The results of paired sample t test indicated that significant difference was found only in gray values ($P< 0.01$), while no significant difference was found in volume and surface of bone geometric models ($P> 0.05$).

Three PMIs around x, y and z axis of metatarsals from two scans are shown in Part V of the supplementary material (Table 4). The paired sample t test was employed to compare the measured PMIs around x, y and z axis of 120 metatarsals' geometric model. The results showed that significant difference was found only in PMIy ($P< 0.05$), whilst no significant difference was found in PMIx ($P> 0.05$) nor in PMIz ($P> 0.05$).

IV. DISCUSSION

In the present study, we reconstructed the geometric models of 120 metatarsals based on anisotropic voxels. Comparison of the results showed that no significant difference was found in geometrical parameters: volume, surface, length, width, height and two PMIs. In addition, variation in ratio of length from two scans was lower than 1%, indicating that there was little difference in the reconstructed bone geometric model based on anisotropic voxels.

So far, the model was successfully employed by researchers for predicting the bone strength, but the possibilities for virtual analysis of human body are enormous.[39] It would be advantage if the CSI obtained during routine radiological imaging may be utilized for such a modeling computer analysis. However, it is of importance to note that scanning as well as reconstruction parameters set by different radiologists may considerably vary. It was the case in the present study. Hence, common sense lead to the arising the question whether those two different set of CSI may be used with the same accuracy for generating 3D models of scanned metatarsal bones. The obtained results are of paramount importance since both types of metatarsal geometric models resulted in, not only linear and volumetric, but even more important, in identical kinematic outcomes. Thus, current results have a potential to overcome a critical hurdle in virtual bone analysis because it is proven that CSI obtained from routine medical examination may be employed for an accurate FEA of metatarsal bones.

In the FEA of bone, some studies used isotropic voxels[40–42] while others used anisotropic voxels.[43,44] The results from both methods were consistent with the actual bone strength.[41,43] Our results suggested that the reconstructed bone geometric model generated by anisotropic voxels could be applied to the FEA when the target bones were included in the entire FOV. Results of the present study are consistent with studies which used anisotropic voxel in finite element analysis and got results highly corresponding to actual bone strength.

It should be noted that some studies showed that the method of femur bone strength prediction using hip axis length of femur was feasible,[45–49] suggesting that our method of acquiring bone length based on bone body coordinates system should have the potential for bone strength prediction because bone length can be obtained automatically by this method. Even considering the anisotropic voxel, the change of bone length is not higher than 1%. One additional advantage of the proposed method is that the length of bone along the long axis can be obtained automatically by the method that sets three PAIs of bone as the body coordinate axes and COM as the origin of the body coordinate system. PAIs of bone are unique, which can avoid the influence of scanning posture on the bone body coordinate system, ensuring high accuracy of the length, width and height of bone. Acquiring bone geometric characteristics based on PAIs has potential to be a new method for evaluating bone strength and this should not be limited in femur evaluation. Although the cost of doing the FEA is higher, it is highly recommended to use the FEA to predict the bone strength, considering the serious consequences of fracture and the subsequent medical costs. In addition, owing to its prominent capacity in analysis and prediction of stress distribution, FEA has an extensive application in clinical medicine fields. Increasing research using FEA are reported to study the stress distribution of tibiofemoral joint and tibiotalar joint for total knee arthroplasty, total ankle arthroplasty and postoperative rehabilitation.[50–54] It has also been employed to investigate the effect of numerous diseases such as diabetes, valgus deformation and tibial and fibular osteotomy on the stress distribution of joints and bones.[55–57]

Overall, the gray values were affected not only by the scanner properties but also by the scanning environment,[58,59] which might lead to a significant difference in gray values from two scans, resulting in the differences of PMI*y*. Nevertheless, in the FEA of bone, the compact bone and the cancellous bone are often regarded as isotropic, suggesting that these differences have little effect on the FEA of bone.

Some limitations of this study should be noted. The FOV parameter was considered as the factor influencing the accuracy of 3D reconstruction without taking both anisotropic and isotropic (control) voxels. This was primarily due to the data collected from patients during routine medical x-ray examination and inability to obtain control isotropic set of the images owing to the ethical issues. The accuracy of both isotropic and anisotropic voxels on 3D reconstructive procedures' accuracy will be tested on phantoms in future investigations. Although only two FOVs were selected, it is to assume that it is highly relevant from the clinical point of view. For instance, during bone tissue engineering procedures for the bone defect reconstruction, it is more sensible approach to use already existing CT patient data than to x-ray patient in order to generate 3D printable geometric models.[60] In line with this, it is also reasonable to stipulate that different radiologists from different medical centers use different scanning settings, among others different FOVs. In the present study, it is proven that they can be used with the same accuracy for the bone 3D reconstructive procedures.

V. CONCLUSIONS

The results of the present study lead to the conclusion that reconstruction of a bone geometric model based on anisotropic voxels caused by FOVs is accurate. One hundred and twenty metatarsals from scans with 2 different FOVs were reconstructed and their geometric models were generated. After comparing the reconstructed models, we found that there was no significant difference in the volume, surface, length, width and height nor in bones' two principal moments of inertia (PMIs). At the sub-millimeter scale, the reconstructed bone geometric models derived from anisotropic voxels are accurate, indicating that applying the reconstructed bone geometric model generated by anisotropic voxels to FEA is reliable. Future studies are encouraged to investigate the bone strength using the generated 3D models.

SUPPLEMENTARY MATERIAL

See supplementary material for the slice parameter information, method applied and related results.

ACKNOWLEDGMENTS

This work was supported by the National Natural Science Foundation of China [Grant no. 11172073, 2017] and Ministry of Education, Science and Technological Development of the Republic of Serbia (grant no. III 45005)

[1] https://www.sheffield.ac.uk/FRAX-DEMO/pdfs/WHO_Technical_Report.pdf.
[2] O. Johnell and J. A. Kanis, Osteoporos Int. **17**, 1726 (2006).
[3] https://www.iofbonehealth.org/compendium-of-osteoporosis.
[4] M. Bessho, I. Ohnishi, J. Matsuyama, T. Matsumoto, K. Imai, and K. Nakamura, J Biomech. **40**, 1745 (2007).
[5] N. Harvey, E. Dennison, and C. Cooper, Nat Rev Rheumatol. **6**, 99 (2010).
[6] U. S. P. S. T. Force, Ann Intern Med **154**, 356 (2011).
[7] E. S. Leib, E. M. Lewiecki, N. Binkley, and R. C. Hamdy, J Clin Dent **7**, 1 (2004).
[8] J. Cunningham, S. M. Sprague, J. Cannata-Andia, M. Coco, M. Cohen-Solal, L. Fitzpatrick, D. Goltzmann, M. H. Lafage-Proust, M. Leonard, S. Ott, M. Rodriguez, C. Stehman-Breen, P. Stern, and J. Weisinger, Am J Kidney Dis. **43**, 566 (2004).
[9] J. Bauer, S. Virmani, and D. Mueller, MedicaMundi **54**, 31 (2010).
[10] P. Hofmann, M. Sedlmair, B. Krauss, J. L. Wichmann, R. W. Bauer, T. G. Flohr, and A. H. Mahnken, Proc. of SPIE 97853E (2016).
[11] G. Guglielmi, C. C. Gluer, S. Majumdar, B. A. Blunt, and H. K. Genant, Eur Radiol. **5**, 129 (1995).
[12] J. H. Keyak, Med Eng Phys. **23**, 165 (2001).
[13] J. S. Gregory and R. M. Aspden, Med Eng Phys. **30**, 1275 (2008).
[14] D. Altkorn and A. S. Cifu, JAMA Clinical Guidelines Synopsis **313**, 1467 (2015).
[15] E. Biver, C. Durosier-Izart, T. Chevalley, B. van Rietbergen, R. Rizzoli, and S. Ferrari, J Bone Miner Res **33**, 328 (2018).
[16] D. D. Cody, G. J. Gross, F. J. Hou, H. J. Spencer, S. A. Goldstein, and D. P. Fyhrie, J Biomech. **32**, 1013 (1999).
[17] R. P. Crawford, C. E. Cann, and T. M. Keaveny, Bone **33**, 744 (2003).
[18] J. A. Macneil and S. K. Boyd, Bone **42**, 1203 (2008).
[19] F. Johannesdottir, E. Thrall, J. Muller, T. M. Keaveny, D. L. Kopperdahl, and M. L. Bouxsein, Bone **105**, 93 (2017).
[20] P. Pottecher, K. Engelke, L. Duchemin, O. Museyko, T. Moser, D. Mitton, E. Vicaut, J. Adams, W. Skalli, and J. D. Laredo, Radiology **280**, 837 (2016).
[21] M. Viceconti, M. Qasim, P. Bhattacharya, and X. Li, Current Osteoporosis Reports **16**, 216 (2018).
[22] E. Schileo, F. Taddei, A. Malandrino, L. Cristofolini, and M. Viceconti, J Biomech **40**, 2982 (2007).
[23] L. Grassi, S. P. Väänänen, M. Ristinmaa, J. S. Jurvelin, and H. Isaksson, J Biomech **49**, 802 (2016).
[24] O. S. Pianykh, *Digital Imaging and Communications in Medicine (Dicom): A Practical Introduction and Survival Guide* (Springer Berlin Heidelberg, 2009).
[25] L. W. Goldman, J Nucl Med Technol **35**, 115 (2007).
[26] S. Poelert, E. Valstar, H. Weinans, and A. A. Zadpoor, Proc Inst Mech Eng H. **227**, 464 (2013).
[27] T. A. Burkhart, D. M. Andrews, and C. E. Dunning, J Biomech. **46**, 1477 (2013).
[28] H. Hu, Medical Physics **26**, 5 (1999).
[29] M. Prokop and M. Galanski, *Spiral and Multislice Computed Tomography of the Body* (Thieme, 2011).
[30] E. K. Paulson, J. P. Harris, T. A. Jaffe, P. A. Haugan, and R. C. Nelson, Radiology **235**, 879 (2005).
[31] T. A. Jaffe, L. C. Martin, J. Thomas, A. R. Adamson, D. M. DeLong, and E. K. Paulson, Radiology **238**, 135 (2006).
[32] B. Vasilic, J. Magland, M. Wald, and F. W. Wehrli, Proc. of ISMRM, 3627 (2008).
[33] J. Rydberg, K. A. Buckwalter, K. S. Caldemeyer, M. D. Phillips, D. J. Conces, A. M. Aisen, S. A. Persohn, and K. K. Kopecky, Radiographics **20**, 1787 (2000).
[34] M. O. Philipp, K. Kubin, T. Mang, M. Hormann, and V. M. Metz, Eur J Radiol. **48**, 33 (2003).
[35] O. Honda, T. Johkoh, S. Yamamoto, M. Koyama, N. Tomiyama, T. Kozuka, S. Hamada, N. Mihara, H. Nakamura, and N. L. Muller, AJR Am J Roentgenol. **179**, 875 (2002).
[36] M. Dewey, A. Lembcke, C. Enzweiler, B. Hamm, and P. Rogalla, Ann Thorac Surg. **77**, 800 (2004).
[37] A. F. Kopp, A. Kuttner, T. Trabold, M. Heuschmid, S. Schroder, and C. D. Claussen, Br J Radiol. **77**(Spec No 1), 87 (2004).
[38] N. C. Dalrymple, S. R. Prasad, F. M. El-Merhi, and K. N. Chintapalli, Radiographics **27**, 49 (2007).
[39] S. S. Pajic, S. Antic, A. M. Vukicevic, N. Djordjevic, G. Jovicic, Z. Savic, I. Saveljic, A. Janović, Z. Pesic, and M. Djuric, Frontiers in Physiology **8**, 493 (2017).
[40] D. Ulrich, B. van Rietbergen, H. Weinans, and P. Ruegsegger, J Biomech. **31**, 1187 (1998).
[41] B. Varghese, D. Short, R. Penmetsa, T. Goswami, and T. Hangartner, J Biomech. **44**, 1374 (2011).
[42] M. Piccinini, J. Cugnoni, J. Botsis, G. Zacchetti, P. Ammann, and A. Wiskott, Comput Methods Biomech Biomed Engin. **17**, 1403 (2014).
[43] J. E. Koivumaki, J. Thevenot, P. Pulkkinen, V. Kuhn, T. M. Link, F. Eckstein, and T. Jamsa, Bone **50**, 824 (2012).
[44] H. Ike, Y. Inaba, N. Kobayashi, Y. Hirata, Y. Yukizawa, C. Aoki, H. Choe, and T. Saito, Comput Methods Biomech Biomed Engin. **18**, 1056 (2015).
[45] W. D. Leslie, L. M. Lix, S. N. Morin, H. Johansson, A. Odén, E. V. McCloskey, and J. A. Kanis, Journal of Clinical Densitometry **19**, 326 (2016).

[46] K. M. Karlsson, I. Sernbo, K. J. Obrant, I. Redlund-Johnell, and O. Johnell, Bone **18**, 327 (1996).
[47] S. Gnudi, C. Ripamonti, G. Gualtieri, and N. Malavolta, Br J Radiol. **72**, 729 (1999).
[48] K. G. Faulkner, W. K. Wacker, H. S. Barden, C. Simonelli, P. K. Burke, S. Ragi, and R. L. Del, Osteoporos Int. **17**, 593 (2006).
[49] W. D. Leslie, L. M. Lix, S. N. Morin, H. Johansson, A. Oden, E. V. McCloskey, and J. A. Kanis, J Clin Endocrinol Metab. **100**, 2063 (2015).
[50] T. L. H. Donahue, M. Hull, M. M. Rashid, and C. R. Jacobs, J Biomech Eng **124**, 273 (2002).
[51] E. Pena, B. Calvo, M. Martinez, and M. Doblare, J Biomech **39**, 1686 (2006).
[52] M. H. Ramlee, M. R. A. Kadir, and H. Harun, Adv Mat Res 183 (2014).
[53] C.-W. Liu, C.-S. Wang, C.-T. Chen, and C.-C. Lo, Adv Sci Lett **4**, 80 (2011).
[54] Y. Wang, Z. Li, D. W.-C. Wong, C.-K. Cheng, and M. Zhang, J Orthop Translat **12**, 55 (2018).
[55] J. T.-M. Cheung, M. Zhang, A. K.-L. Leung, and Y.-B. Fan, J Biomech **38**, 1045 (2005).
[56] L. Blecha, P. Zambelli, N. Ramaniraka, P.-E. Bourban, J.-A. Månson, and D. P. Pioletti, Comput Method Biomech **8**, 307 (2005).
[57] Y. Zhang, J. Awrejcewicz, O. Szymanowska, S. Shen, X. Zhao, J. S. Baker, and Y. Gu, Comput Biol Med **97**, 1 (2018).
[58] C. Levi, J. E. Gray, E. C. McCullough, and R. R. Hattery, AJR Am J Roentgenol. **139**, 443 (1982).
[59] R. Groell, R. Rienmueller, G. J. Schaffler, H. R. Portugaller, E. Graif, and P. Willfurth, Comput Med Imaging Graph. **24**, 53 (2000).
[60] A. A. Egorov, A. Y. Fedotov, A. V. Mironov, V. S. Komlev, V. K. Popov, and Y. V. Zobkov, Beilstein J Nanotechnol **7**, 1794 (2016).